HYDRATION IN TWO-DIMENSIONAL SYSTEMS

Lisbeth Ter-Minassian-Saraga

Physico-Chimie des Surfaces et des Membranes, Equipe de Recherche du CNRS associée à l'Université Paris V, UER Biomédicale, 45 rue des Saints-Pères, 75270 Paris cedex 06, France

Abstract - The melting of the structural water in multibilayer systems is investigated by means of true differential scanning calorimetry in the range - 60°C to + 80°C. Freezing experiments have been carried out too.
The multibilayer systems consist in aqueous dispersions of phospholipids at various phospholipid/water amounts or in (phospholipid + additive) dispersed in a given amount of water (40% - 60% w/w) for various phospholipid/additive amounts.
The phospholipids are DPPC (1-2-dipalmitoyl-sn-glycero-3-phosphocholine), PI (phosphatidylinositolmonophosphate from wheat) and egg lecithin E-L. The additives are cholesterol Ch, vinblastine VLB and a hydrophobic charged macromolecule (polysoap PS). From the melting thermograms the apparent heat of melting L of the structural water inside the aqueous separation is deduced. It is evident that the additive affects specifically both the structural water and the bilayer thermodynamic behaviour. This result is compared mainly with results of studies of phospholipids swelling in water under various conditions and also to condensation in mixed monolayers.

INTRODUCTION

Cell-cell, vesicle cell and vesicle-vesicle fusion require contact between membranes beyond the membranes "wall" of hydration (Ref.1-4). This "wall" consists of water molecules bound by the membrane components located on the external face of the membranes.

In multilamellar or multibilayer aqueous phospholipid systems these bound (Ref.5,6) or structural water molecules produce the repulsive hydration force or pressure (Ref.1,2) which is decomposed (Ref.3) in its normal and lateral constituents.

The effect of cholesterol on the structural water of lecithins has been noticed in Ref.6. The effect of cholesterol on the state of natural and of synthetic phospholipids has been studied intensively. Various spectroscopic technics have been used to study the dynamic state and the organization of the lipid molecules in bilayers (Ref.7,8). Cholesterol acts as an impurity in the bilayers (Ref.9) but the amount of its incorporation is limited (Ref.6). The acyl groups are ordered by cholesterol according to Ref.10. They are disordered according to Ref.11. Raman studies detect a change in acyl group conformation and in the stretching mode frequency of the esters carbonyls (Ref.12 ,13). The contribution of hydrogen bonds to the polar head region of the bilayers and monolayers has been emphasized (Ref.14,15). Polar head group mobility of DPPC is increased by small amounts of cholesterol molecules acting as "spacers" (Ref.17). Water molecules also act as spacers as they increase the area per DPPC molecule (Ref.13, 17). When the composition of the system is 5/1 (molecule/molecule) water/lipid, water extends up to the glycerol back bone (Ref.16). Hydrogen bond formation between the β-OH of cholesterol and the ester carbonyl of the phospholipid (Ref.13) is not observed. The contradictory effect of cholesterol on EL and DPPC in either bilayer or monolayer state (Ref.7) is not understood yet. In particular the "spacer" behaviour of cholesterol in bilayers contradicts its condensing effect in mixed monolayers with DPPC (Ref.18,19).

The amount of water associated with the polar groups in monolayers cannot be determined.

Recently, an indirect method for studying hydration in monolayers has been
suggested (Ref.20).

In bilayers the results obtained for lipid hydration may vary with the tech-
nique used to determine it. DSC used first in Ref.6 has revealed the class
of "non freezing" water : in multibilayer systems we find (Ref.21) that
phospholipid multibilayer systems include also a class of water molecules
freezing and melting below 0°C. These molecules and the non freezing ones
constitute the aqueous separation between bilayers and are affected by the
surface forces of the bilayers. When the composition of the bilayers changes
the surface forces are modified. The hydration or the amount of the two
classes of water inside the aqueous separation is affected. For phospholipids,
the "spacer" effect of water molecules has been found by X-Ray analysis
of lamellar systems (Ref.1-3 & 22,23).

A similar "spacer" behaviour of water bound to phospholipid polar heads has
been observed recently for natural membranes using neutron diffraction. These
membranes include proteins (Ref.24,25).

Calorimetry cannot provide a resolved picture of water binding to the phos-
pholipid bilayers. The results of calorimetric studies are complementary to
the isothermal studies of hydration forces (Ref.1-3) by X-Ray and ultra-
filtration.

Before reporting our results we compare the behaviour of multibilayers on iso-
thermal ultrafiltration and on isobaric cooling or heating below 0°C.

ULTRAFILTRATION WITH /ICE MELTING AND WATER FREEZING/ IN WATER SWOLLEN PHOSPHOLIPIDS

Phospholipid hydration and swelling at constant temperature, pressure and volume

In a reference state pure dry bulk lipid and pure bulk water occupy separate
volumes V_l^b and V_w^b such that $V = V_l^b + V_w^b$ at the reference temperature T_a and
pressure p_o = 1 atm (Fig.1a). The lipid water interface is negligible. In the
equilibrium swollen state (Fig.1b) this interface has increased and n_w^σ moles
of excess water have been added to maintain V_w^b constant, assuming V_l^b is
unchanged on swelling. This amounts to a change in water density next to the
bilayer surface. Also it implies that the aqueous spacings occupy the volume
V_w^b which is filled with "bulk" water, the excess water beeing located on the
ideal lipid/water plane interface (Gibbs convention).

In short, the Gibbs convention is equivalent to assuming that the water
swollen lipid WSL consists in pure dry lipid, bulk water and adsorbed water.

The occurence of the equilibrium water spacing h_w is the result of the
balance between the attractive and the repulsive interbilayer forces (springs
in Fig.1b and 1c).

The differential of the internal energy of the system in Fig.1b is equal to :

$$dU = TdS - pdV + \mu_l\, dn_l + \mu_w\, dn_w + 2\, \sigma dA - A\, \Pi\, dh_w \qquad (1)$$

where S, μ_i, n_i, σ, A, Π, designate entropy, chemical potential and number
of moles of constituent i, water w and lipid l, the interfacial tension and
area and the net pressure (force/unit area) resulting from various inter-
actions between bilayers.

The Gibbs free energy G defined at given T, p, σ, h_w is obtained from (1)
(Ref.26, Ch.XII). It is equal to :

$$G = U - TS + pV - 2\sigma A = \tilde{G} - 2\sigma A = n_l\, \mu_l + n_w\, \mu_w \qquad (2)$$

From (1) and (2) the chemical potential of water in the system at equilibrium
is obtained as in Ref.26 (eq.12.7 to 12.14) :

$$\mu_w = \left(\frac{\partial G}{\partial n_w}\right)_{T,p,\sigma,n_j,h_w} \qquad (j \neq w) \qquad (3)$$
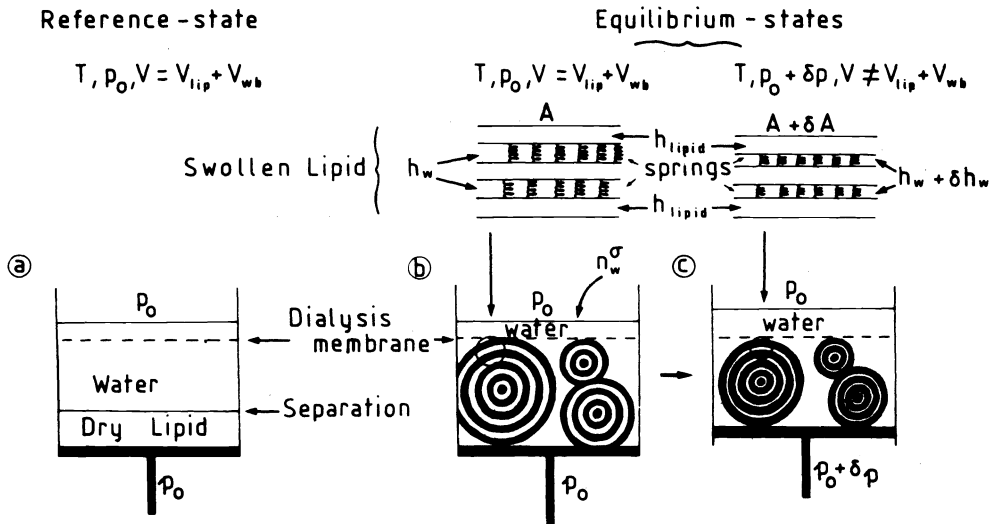
Reference - state

$T, p_O, V = V_{lip} + V_{wb}$

Equilibrium - states

$T, p_O, V = V_{lip} + V_{wb}$ $T, p_O + \delta p, V \neq V_{lip} + V_{wb}$

Fig.1. Isothermal ultrafiltration (Ref.3).
(a) Reference state at temperature T and pressure p_O.
(b) Equilibrium at T, p_O; equilibrium at T, $p_O + \delta p$ (c).
V, V_{lip}, V_W volumes occupied by all the condensed phases, by the dry
lipid and by bulk water respectively.
n_W^σ : adsorbed water (moles). "Onions" = multibilayers.
Enlarged sections : A = total bilayer area ; h_W = L aqueous spacing
width ; springs = model of net force/unit area Π between bilayers
(Π = 0 for δp = 0). h_{lip} = bilayer thickness.

Isothermal ultrafiltration experiment (Ref.3).
The system in Fig.1b is open with respect to water and closed with respect
to the lipid; dn_1 = 0 in eq.1). At a given T and n_1 the pressure on the
piston is brought to $p_O + \delta p$. In this situation (Fig.1c) water is in dif-
fusion equilibrium at two pressures p_O and $p_O + \delta p$ on the two sides of the
dialysis membrane. Therefore :

$$\mu_W (T, p_O) = \mu'_W (T, p_O + \delta p) \tag{4}$$

Why water is at equilibrium at two different pressures ? From (1) and (2),
the following differential of G is obtained :

$$dG = - SdT + Vdp + \mu_1 dn_1 + \mu_W dn_W - 2Ad\sigma - A\Pi dh_W \tag{5}$$

Cross differentiation of (5) leads to :

(a) $\left(\dfrac{\partial \mu_W}{\partial \sigma}\right)_{T,p,n_1,h_W,n_W} = - 2\left(\dfrac{\partial A}{\partial n_W}\right)_{T,p,n_1,h_W,\sigma}$

(b) $\left(\dfrac{\partial \mu_W}{\partial h_W}\right)_{T,p,n_1,\sigma,n_W} = - A \left(\dfrac{\partial \Pi}{\partial n_W}\right)_{T,p,n_1,\sigma,h_W}$ $\tag{6}$

(c) $\left(\dfrac{\partial \mu_W}{\partial p}\right)_{T,n_1,\sigma,h_W,n_W} = \left(\dfrac{\partial V}{\partial n_W}\right)_{T,n_1,\sigma, h_W,p} = v_W(T,n_1,\sigma,h_W,p)$

Comparing the chemical potentials of water in Fig.1b and in Fig.1c, for small
δp, $\delta\sigma$, δh_W, δn_W we have :

$$\delta\mu_W = 0 = (\frac{\partial\mu_W}{\partial p})_{T,\sigma,h_W,n_1,n_W}\delta p + (\frac{\partial\mu_W}{\partial h_W})_{T,p,\sigma,n_1,n_W}\delta h_W + (\frac{\partial\mu_W}{\partial\sigma})_{T,p,h_W,n_W,n_1}\delta\sigma \qquad (7)$$

Using the cross coefficients (6) we obtain from (7) :

$$v_W\,\delta p = 2(\frac{\partial A}{\partial n_W})_{T,p,n_1,h_W,\sigma}\delta\sigma + A(\frac{\partial\Pi}{\partial n_W})_{T,p,n_1,\sigma,h_W}\delta h_W \qquad (8)$$

Therefore the flow work ($v_W\,\delta p$) and δp measured in Ref.3 have one contribution from the lateral extension of area due to hydration of the lipid bilayers i.e. ($\partial A/\partial n_W$), the first term of the l.h.s. of eq.8, and one contribution from the change in the aqueous separation h_W which affects the net pressure Π. This pressure is the resultant of opposed dispersion and hydration forces which vary with h_W (Ref.3).

<u>Effect of lipid bilayers on ice-water transition inside the aqueous separation between them. Cryoscopic experiments at constant pressure.</u>
We are interested in the depression of water-ice transition temperature inside the aqueous separation between bilayers.

It has been assumed (Ref.27) that surface forces shift or modify the free energy of water at given T and external pressure p_0 but not that of ice. For $T > T_a$, this shift $\delta\tilde{\mu}^W_{T,p_0}$ of the water molar free energy has been expressed as a power law of the distance from the lipid bilayer interface (Ref.21).

$$\delta\tilde{\mu}^W_{T,p_0,L} = -\frac{a}{y^\alpha}\{1 + \frac{y^\alpha}{(L-y)^\alpha}\} = -\frac{a}{y^\alpha}\,\phi\,(L,y),\quad T > T_a \qquad (9)$$

where $L \equiv h_W$ and a, α are adjustable parameters. $T_a = 0°C$ is the normal ice water transition temperature. The factor ϕ accounts for the overlapping of two bilayers effects on the water molecules inside the aqueous gaps.
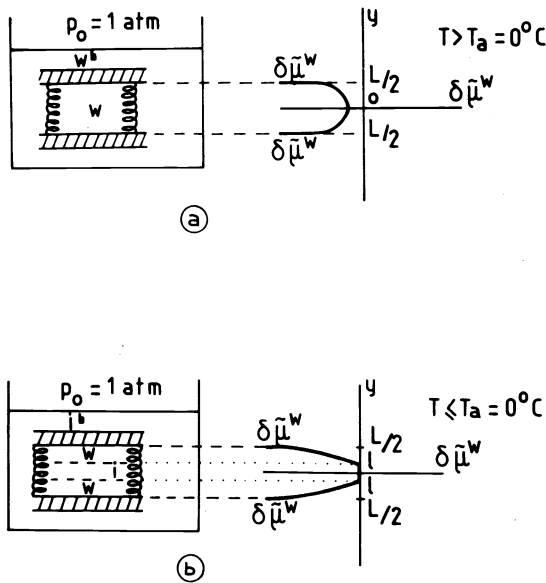

Fig.2. Aqueous spacing between bilayers at p_0 and either above or below $T_a = 0°C$.
a) w^b,w = bulk water, internal water (inside aqueous spacing); L = width of aqueous spacing; y = distance from bilayer water interface. Springs: as in Fig.1. $\delta\tilde{\mu}^W$= shift of water molar free energy for internal water.
b) i^b,i = bulk ice, internal ice; ice-water interface at y = 1.
c) qualitative plots of $\delta\tilde{\mu}^W$ and of $\delta\tilde{\mu}^i$ vs y at three temperatures $T < T_a$; l_1, l_2, l_3 corresponding equilibrium positions for the ice water front.
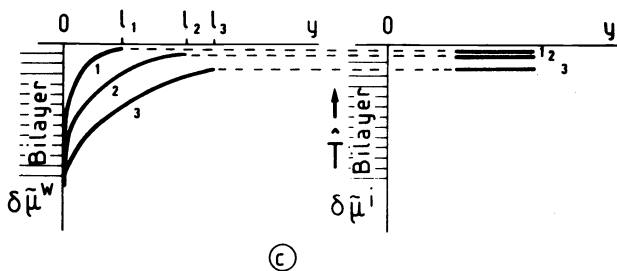
The equilibrium condition between ice on top of the dialysis membrane in Fig.1, at $T < T_a$ and $p_0 = 1$ atm, and water or ice inside the aqueous separation when the position of the ice water interface is $y = 1$ (Fig.2) recquires that :

(a) $\quad \mu^i_{p_0,T} = \mu^{io}_{p_0,T_a} - \int_0^{\hat{T}} s^i \, dT + v^i(p^i - p_0)$

(b) $\quad \mu^W_{p_0,T,L} = \mu^{W,o}_{p_0,T_a} - \int_0^{T-T_a} s^W \, dT - \frac{a}{1^\alpha} \phi \, (L,1) + v^W(p^W - p_0)$ (10)

(c) $\quad \mu^i_{p_0,T} = \mu^W_{p_0,T,L}$ at $p^i = p^W = p^o$, $h_W = L$ and $y = 1$.

The shift $\hat{T} = T - T_a < 0$ is the displacement of the ice transition temperature for $y = 1$. At constant L, $s^W - s^i = \Delta s$ is the molal entropy of ice melting at $p = p_0$ and $T = \hat{T} + T_a$. Defining the average molal enthalpy of ice melting at p_0 as L where :

$$ L = \int_0^{\hat{T}} (s^W - s^i)_{p_0,h_W,A} \, dT \simeq \frac{L(p_0,T_a)}{T_a} \hat{T} \tag{11} $$

We obtain the variation of l with temperature from (10) and (11) :

$$ \frac{L}{T_a} \hat{T} + \frac{a\phi(1,L)}{1^\alpha} = 0 \tag{12} $$

The relation between the position l of the ice water interface inside the aqueous separation and the depression $\hat{T}$, is shown in Fig.2. At large shifts $\hat{T}$, T and l are small. This implies that melting of ice *starts at the ice bilayer interface and proceeds towards the midplane of the separation* $L \equiv h_W$. When l = L/2 melting ends and $\hat{T} = \hat{T}_{min}$. When $1 = 1_0$ and $1 = (L - 1_0)$ let $\hat{T} = \hat{T}_{max}$. Melting starts when $\hat{T} \simeq \hat{T}_{max}$. From (12) we have :

(a) $\quad -\hat{T}_{min} = 2^\alpha \dfrac{T_a}{L} \dfrac{a\phi(L/2)}{L^\alpha} \neq 0$

(b) $\quad -\hat{T}_{max} = \dfrac{T_a}{L} \dfrac{a\phi(1_0,L)}{1_0^\alpha}$ (13)

(c) $\quad \dfrac{\hat{T}_{max}}{\hat{T}_{min}} = \dfrac{\phi(1_0,L)}{2^\alpha \phi(L/2)} (\dfrac{L}{1_0})^\alpha \simeq \dfrac{1}{2^\alpha \phi(L/2)} (\dfrac{L}{1_0})^\alpha$

when $1_0 \ll L$, $\phi(1_0, L) \to 1$ (see eq.9). $\hat{T}_{min} \to 0$ when $L \to \infty$ for $\alpha > 1$. Also, when $1_0 \to 0$, $(L - 1_0) \to 0$, $\hat{T}_{max} \to \infty$. According to eq.1, we assume that melting takes place at constant $h_W \equiv L$ and area A.

From (12) and (13), the relative rate of displacement of ice water interface with temperature at given p_0, L and A are obtained as a function of the temperature shift $\hat{T}$:

$$ \{\frac{d(1/L)}{d\hat{T}}\}_{p_0,L,A} = \frac{1}{2} \frac{d}{d\hat{T}} \left[\{\frac{\phi(1/L)}{\phi(L/2)} (-\hat{T}_{min})\}^{1/\alpha} \frac{1}{(-\hat{T})^{1/\alpha}} \right] \tag{14} $$

When (14) is multiplied by the mass of ice melting inside the aqueous separation of the bilayers of Fig.1b and by the average enthalpy of ice L melting defined at given p_0, A, h_W we obtain the temperature rate of melting of ice inside the aqueous separation. In the experiment in which the temperature of the WSL increases with a given time rate $\hat{T}_p$, eq.14 predicts a time rate variation of the relative position (1/L) of the ice water interface. If (L/18) is the enthalpy of melting per gram of water, the rate of heat absorption per unit time by the mass m_s of water gradually melting inside the aqueous separation at constant p_0, h_W, A is equal to

$$ (\frac{dQ}{dt})_{p_0,h_W,A} \simeq \frac{m_s L \hat{T}_p}{18 \, \alpha} \{\frac{\phi(1/L)}{\phi(L/2)} (-\hat{T})_{min}\}^{1/\alpha} (-\hat{T})^{-(\alpha+1)/\alpha} = \epsilon \tag{15} $$

This rate of heat exchange corresponds to simultaneous melting of ice on both bilayers boarding one aqueous space. When ice melting is coupled with

spontaneous increase in bilayer area A or spacing $h_w = L$, the measured
$(dQ/dt)_{p_o}$ includes effects in addition to those predicted by eq.15.

Apparent molar enthalpy of ice-water transition. Non-freezing, non-melting
water molecules and hydration of bilayers.
The linear plot log $(dQ/dt)_{p_o}$ vs log $(-\hat{T})$ may provide the value of the para-
meter α of eq.9 for surface forces. Such a linear plot may be obtained only
when variations of A and L contribute very little to the head absorbed on
ice melting.

The integral of (15) with respect to the time provides $Q = L \quad (m_s/18)$ the
apparent value of L . This factor may be obtained also from the
measurements of (dQ/dt) and eq.15 when α is known and $\phi(1/L) \rightarrow \phi(L/2)$. When
the value of Q is smaller than $(m_s/18)L$, it is assumed that the aqueous
separation has two classes of water molecules : the normally melting ones for
which $L \simeq 1440$ cal mol^{-1} (Ref.28) and the non-freezing non-melting water
molecules for which $L = 0$. Such a distribution of water molecules in lamellar
systems is consistent with the simple Gibbs convention (see section a). When
the non-freezing non-melting water molecules   form layers of thickness
$l = l_o$ next to the bilayers (Fig.3), this thickness corresponds according to
eq.12 to a large value T_{max} for the temperature shift of the ice water tran-
sition temperature. For $|\hat{T}| > |\hat{T}_{max}|$,(dQ/dt) = 0. The heat of ice melting Q
obtained from the integral of (15) is then equal to

$$Q = \frac{m_s L}{18} \left(1 - \frac{2l_o}{L}\right).$$ (16)

It corresponds to a "spectrum" of ice/water transition temperature shifts in
the range $\hat{T}_{max}$ to $\hat{T}_{min}$. In the case of increased interaction between bilayers
and water (increased hydration) l_o increases, Q and $\hat{T}_{max}$ decrease according
to (16) and to (12) respectively.

Ultrafiltration in monolayers and lateral pressure in bilayers.
Compressing a spread monolayer of lipid in a Langmuir trough is a two-
dimensional ultrafiltration at constant μ_w as in Fig.1b and Fig.1c. For the
monolayer $h_w = \infty$, $\Pi = 0$, in (5) and in (1) n_1, p, T, σ and the chemical
potential of water μ_w are fixed. The area $A = A_o + A_f$ of the substrate
consists of the clean surface A_o of surface tension σ_o and of the surface
covered film A_f of surface tension σ_f. To transfer δn_w moles of water from
the area A_f into the area A_o at constant σ_f and σ_o, μ_w, T, p a two-dimen-
sional, isothermal flow work is performed to compensate the difference in
partial molar free energies of water $\bar{F}_w$ in the area A_f and in A_o. Therefore
from (1), the change in free energy defined as $\delta F = \delta(U - TS)$ is equal to :

$$\delta F_{T,p,n_1,\mu_w,h_w=\infty} = (\bar{F}^\sigma_{w,o} - \bar{F}^\sigma_{w,f})\, \delta n_w = -(\sigma_o - \sigma_f)_{T,p,n_1,\mu_w}\, \delta A_f \quad (17)$$

If we let $\delta A_f/\delta n_w = (\partial A_f/\partial' n_w)_{T,p,n_1,\mu_w}$ in eq.17 we obtain for the change
in the partial molar free energy of transferred water the expression :

$$(\bar{F}^\sigma_{w,o} - \bar{F}^\sigma_{wf}) = -\Delta\sigma \left(\frac{\partial A}{\partial n_w}\right)_{T,p,n_1,\mu_w,\sigma} \quad (18)$$

The difference between the "lateral" pressure in lipid bilayers postulated
in Ref.29 and the usual, monolayer surface pressure is evident by comparing
(8) and (18). While both concepts involve hydration of lipid bilayers or of
monolayers under the same conditions i.e. $(\partial A/\partial n_w)_{T,p,n_1,\mu_w,\sigma}$ is the same,in
one case (eq.8) the lateral pressure is related to exchange of molecules
between an interface and bulk water ; in the other case (eq.18) the surface
pressure is related to exchange of water between two aqueous surfaces. On
both cases the water chemical potential is fixed. However the reference state
is different.

The chemical potential of water μ_w in the surface phase in the presence or in
the absence of the film is obtained from (17) using the definition of partial
molar area of water at the surface ω_w :

$$\overline{F}^{\sigma}_{w,o} - \sigma_o\,\omega_w = \overline{F}^{\sigma}_{wf} - \sigma\omega_w = \mu^o_w(p,T) \qquad (19)$$

where in the monolayer model (Ref.25, eq.12.15) ω_w is defined as follows :

$$(\frac{\partial A}{\partial n_w})_{T,p,\sigma,n_1,\mu_w} = \omega_w(T,p,\sigma) \qquad (20)$$

Freezing of water and ice nucleation between lipid bilayers.
When the system in Fig.1 is cooled below $T = T_a$ which is the normal freezing point of water, assuming supercooling has been avoided, ice has replaced water above the dialysis membrane. Under equilibrium conditions of the system the problem is that of coexistence of external bulk ice with both ice and water inside the aqueous separation between bilayers (Fig.2b).
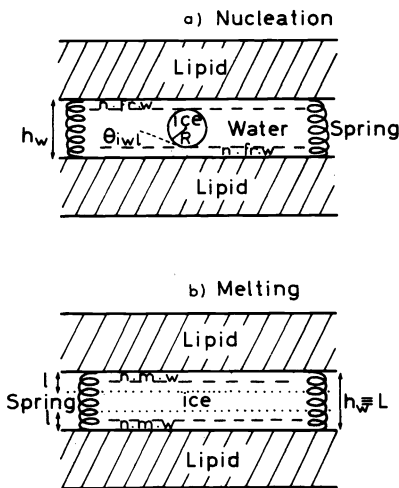

Fig.3. Ice nucleation and ice melting between lipid bilayers.
a) Nucleation. $L = h_W$ aqueous gap width; R = ice nucleus radius; Θ_{iwl} = contact angle; n_{fw} = non freezing layer l_o in eq.16.
b) Ice melting. l = distance of ice water front from bilayer interface. n.m.w = non melting water layer l_o in eq.16.

However freezing by itself proceeds and propagates from an ice nucleus of critical size (Ref.30). It is assumed that the critical diameter of spherical nuclei formed at a given $T < T_a$ inside a porous solid saturated with a liquid (Fig.3) is equal to the effective radius R of a nuclei and is smaller than the real pore radius R_p (Ref.31 & 32). The temperature $T = T_a + \hat{T}$, the equilibrium temperature of ice nucleation in a pore is obtained assuming that the Laplace pressure $(p^i - p^w) = \hat{p}$, where $\hat{p}$ is the pressure shift between ice and water, and the isothermal enthalpy of melting are related by :

$$p_i - p_w = \hat{p} = \frac{2\sigma_{iw}}{R_n} = -\int_{T_a}^{T} \frac{s_w - s_i}{v_i}\,dT \qquad (21)$$

Terms based on Laplace pressure are absent from (12) which is representative of planar systems with $R_p = \infty$. In Ref.30 & 31 the contribution of ice water transition on s_{sup} the entropy of condensate pore forming substance interface is allowed for. The molar enthalpy of the nucleus formation is then equal to :

$$\Delta H_{T,R_n} = T\,\Delta s\,\{1 + \frac{d\sigma_{iw}}{dT}\cos\Theta_{iw}\frac{T}{\sigma_{iw}}\} \quad \text{at } T = T_a + \hat{T} \qquad (22)$$

where σ_{iw} is the ice water interfacial tension, Θ_{iw} is the contact angle of the ice water meniscus with the bilayer surface and Δs is the molar entropy of freezing in bulk at T and $p = p_o + \hat{p}$. The difference between R_p and R is equal to :

$$R_p = R + l_o \qquad (23)$$

where l_0 is the parameter related to $\hat{T}_{max}$ appearing in eq.16. Assuming $\Theta_{iw} = 0$ and using their results for the depression of ice formation from water saturating calibrated porous solids, the variations of $\Delta s = s_w - s_i$ with T and R and of σ_{iw} with T have been deduced in Ref.32 (eq.17 and Fig.2). It is found that the enthalpy of ice water transition in bulk is lowered by about 1% per 1°C depression ($-\hat{T} = 1°C$). This correction of L becomes important for large temperature shifts. Surface effects related to $(d\sigma_{iw}/dT)$ produce additional lowerings of the apparent enthalpy of freezing in porous materials. For water freezing at -20°C, an apparent enthalpy of about 200 J g^{-1} is predicted instead of the normal 332 J g^{-1}. For ice melting at the same temperature the apparent enthalpy (~ 165 J g^{-1}) is lower than the freezing enthalpy under normal conditions.

EXPERIMENTAL AND RESULTS

Materials and apparatus.
Sodium phosphatidylinositolmonophosphate PI extracted from wheat and egg lecithin EL (both Lipid Products), dipalmitoyl lecithin DPPC (Fluka) and cholesterol (Merck) are commercial products. The lipids are tested by TLC. Vinblastine VLB and polysoap PS or PVPC6, 2-methyl-5-vinyl-1-hexylpyridinium bromide are gifts from Eli-Lilly (USA) and from Cl. Loucheux (Lille) respectively. They were used as received.

DSC sample preparation.
Solutions of phospholipid in methanol/chloroform (1/9, v/v) were prepared. Aliquots deposited in aluminium DSC cups are evaporated under a N_2 stream to constant weight ($\pm$ 5 µg). A weighed amount ($\pm$ 5 µg) of water is added. The cup is sealed and reweighed. Cups which loose weight (water) during subsequent treatments are discarded. The lipid pure or mixed with the second constituent weighs 0.5 mg to 2.5 mg. The water weighs 0.25 mg to 1.9 mg. The samples may be incubated at 60°C to $\sim$80°C for periods up to 32h to $\sim$80h when necessary. They were doubled at least.

A Du Pont de Nemours Thermal Analyser and DSC calorimeter type 990-910 equipped with a 990 Mechanical cooling Accessory is utilised either to perform controlled heating experiments or controlled heating-cooling cycles. In general the rate of temperature variation is $\dot{T}_p = 2°$ min^{-1} and the sensitivity is in the range 48-238 µcal sec^{-1}. In our true differential calorimetric exploitation of the apparatus a "water" reference is opposed to the sample. The reference serves also to calibrate the apparatus around and below 0°C.

Thermograms.
Thermograms for heating runs and for cooling-heating cycles are obtained between various temperature limits : - 65°C to 20°C for samples including PI or EL ; - 65°C to 50°C (or 70°C when necessary) for samples including DPPC ; - 65°C to about 0°C or 1°C for the study of water nucleation in the absence of supercooling. Examples of thermograms are shown in Fig.4, in Fig.5 and in Fig.6.

Fig.4 shows typical thermograms for freezing cooling cycles limited at about 0°C. The ice melting (respectively water freezing or nucleation) peaks of the samples occur on the endothermic (exothermic) sides of the thermograms. For reference R the peaks location is reversed. Supercooling in the reference water produces spurious R peaks (Fig.4, $x_{DPPC} = 1$). Such effects are never observed for ice nucleation peaks S of the sample. The peaks S for cooling are sharp. They occur at temperatures T_f easy to locate (see all S peaks on cooling in Fig.4). This location is reproducible ($\sim \pm 1°C$) and independent of supercooling i.e. upper temperature limit of the cycle. The very different aspect of the peaks S : broad for ice melting, very sharp for freezing, has to be emphasized. It is very important.

The Fig.5 represents the following heating thermograms :

a) Sample cup is empty ; the mass of reference water m_{rg} is used to calibrate the apparatus assuming an enthalpy equal to 1440 cal mol^{-1} for the ice-water transition. The location of the peak positions the temperature 0°C as shown.
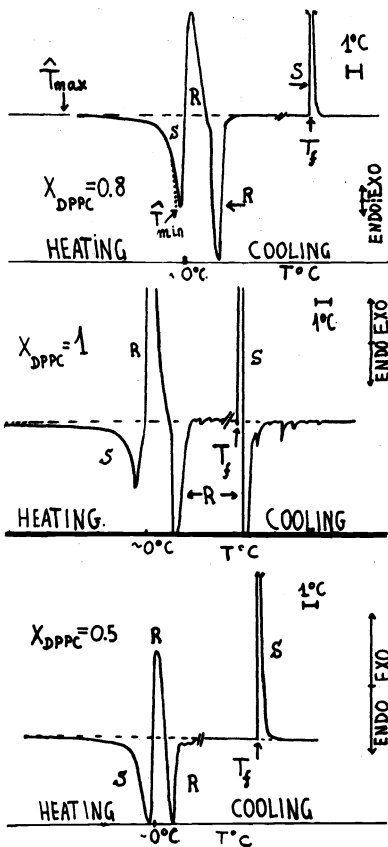
Fig.4. Heating-cooling cycles between -60°C to ∿0°C. (DPPC + VLB) + H_2O (50% w/w). x_{DPPC} = mol fraction of the lipid in the dry mixture. S = sample peaks ; R = reference peaks. T_f = freezing (ice nucleation) temperature. $\hat{T}_{min}$: see eq.13a. $\hat{T}_{max}$: see eq.13b. Dashed curve (x_{DPPC} = 0.8) extrapolated according to eq.15.
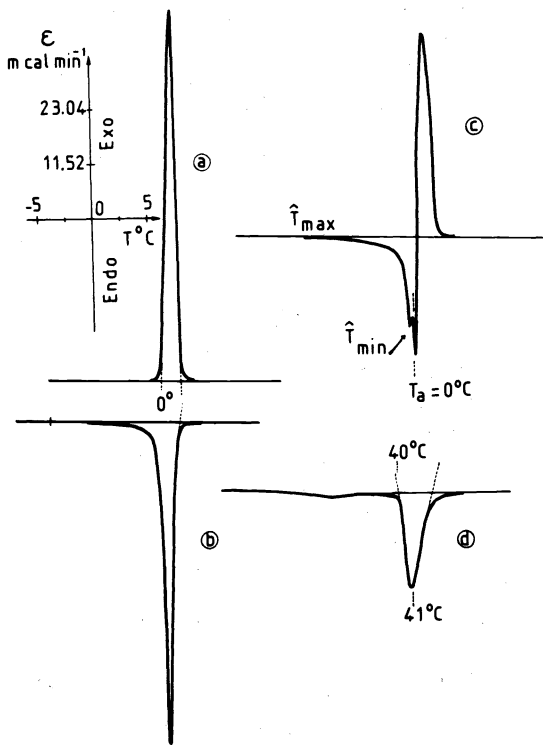

Fig.5. Heating thermograms for fully hydrated DPPC. Heating rate 2°C min^{-1}. 50% (w/w) water.
a) 0.520 mg H_2O in reference cup. Sample cup empty.
b) Sample 0.5 mg DPPC + 0.52 mg H_2O.
c) True DSC technique : (a) and (b) opposed.
d) DPPC gel-liquid crystal transition and pretransition.

b) Reference cup is empty. The peaks of external ice and internal ice melting merge and a broad peak is obtained for ice melting in the sample (compare (a) and (b) peaks in Fig.5). Mass of water in the sample is m_{sg}.

c) Reference (a) and sample (b) ($m_r = m_s$) are opposed (true differential condition). The contribution of the external ice melting in the sample is eliminated. The small peak at $\hat{T}_{min}$ corresponds to the end of internal ice melting (Fig.2), (Ref.21). This $\hat{T}_{min}$ and the $\hat{T}_{min}$ in Fig.4 are comparable. In this last case the external water may not have melted. Both values of $\hat{T}_{min}$ ($\neq$ 0) are different from naught.

Peaks (d) in Fig.5 represent the pretransition and the gel-liquid crystal transition of fully hydrated DPPC.

The thermograms in Fig.6 show a heating-cooling cycle in the range -60°C to 50°C for the mixture (DPPC + VLB) at x_{DPPC} = 0.8. Reference water R super-cooling is evident. The base of the freezing peak S is distorted when compared to the one in Fig.4 for the same sample. The reason of this distortion is not clear. It might be due to some supercooling of internal water.
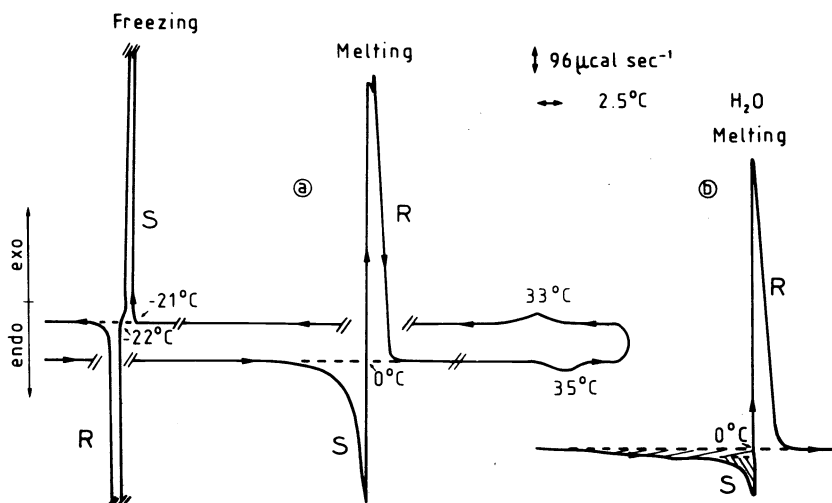

Fig.6. Thermograms for (DPPC + VLB) and for EL.
a)   Heating cooling cycle between -60°C and 50°C. 0.5 mg (DPPC + VLB) + 0.5 mg H_2O. x_{DPPC} = 0.8 (lipid mol fraction in the dry mixture). S = H_2O sample peaks; R = H_2O reference peaks; DPPC transition peaks at 35°C and 33°C. b) Heating thermograms for fully hydrated EL (0.5 mg lipid, 0.5 mg H_2O).

The inset heating thermogram has been obtained for fully hydrated EL (Fig.6).

The systems for which thermograms have been obtained are quoted in Table 1.

Enthalpies of phase transitions in the sample. Freezing and non-freezing water molecules.

The heat exchanged on phase transition by the sample is obtained from the areas of the thermograms peaks. They are measured with a planimeter. We designate by $\Sigma_{H_2O}^{refo}$, $\Sigma_{H_2O}^{ref}$, Σ_{H_2O} the areas corresponding to the ice water transition in the reference cup on calibration (run a, no sample, Fig.5), in the reference cup opposed to sample (in run c, Fig.5) and inside the sample (broad peak at T < 0°C, run c, Fig.5) respectively.

TABLE 1. Systems studied by true DSC

Lipid system	Composition x_{lipid}	% H_2O (w/w)	Thermogram Mode	Rate (°C min^{-1})
DPPC + PVPC6	0 - 1	50	Heating	5
PI + PVPC6	0 - 1	40	"	5
DPPC	1	15,50	"	2
PI	1	15,20,40,60	"	2
EL + Ch	0,0.5,1	50	"	2
DPPC + Ch	0,0.25,0.75,1	50	"	5
DPPC + VLB*	0.25 - 1	50	"	5
DPPC + VLB	0.4 - 1	50	Cycle	2

*(Ref.33) x_{lipid} = mol fraction of lipid

The ratio $\Sigma_{H_2O}^{ref}/\Sigma_{H_2O}^{refo}$ provides the water percentage which does not melt at 0°C
i.e. the percentage of *internal water*. The weight of this water m_s may be
obtained by dividing the heat corresponding to $\Sigma_{H_2O}^{ref}$ by the specific heat of
ice water transition ℓ cal g^{-1}. The number of H_2O moles is obtained from
m_s.

The ratio $\Sigma_{H_2O}^{s}/\Sigma_{H_2O}^{refo}$ is the percentage of internal water undergoing freezing
and melting. The ratio $(\Sigma_{H_2O}^{ref} - \Sigma_{H_2O}^{s})/\Sigma_{H_2O}^{refo}$ is the percentage of water which
neither freezes nor melts in the sample. Out of phase melting of external
water produces the peak on the right of the one located at $\hat{T}_{min}$ on Fig.5c.
The area of this peak, absent from the thermogram of Fig.4 represents less
than 5% of the area $\Sigma_{H_2O}^{refo}$.

When the upper limit of the heating cooling cycle is about 1°C, ice in R has
melted completely. The areas $\Sigma_{H_2O}^{ref}$ of the two peaks R (melting and freezing)
(ex : see Fig.4) are then equal. It is very important to note that although
the shapes of the peaks S for melting and for freezing respectively are very
different (Fig.4) their areas are comparable. For $x_{DPPD} = 0.5$, $\Sigma_{H_2O}^{s}$ (melting)=
8.1 sq cm ; $\Sigma_{H_2O}^{s}$ (freezing) = 8.1 sq cm. For $x_{DPPC} = 0.8$, $\Sigma_{H_2O}^{s}$ (melting) =
8.0 sq cm ; and $\Sigma_{H_2O}^{s}$ (freezing) = 8.17 sq cm. In contrast, when heating is
stopped below 0°C the area of the ice melting peak is smaller than that for
the freezing peak. The behaviour of the water saturating a porous mineral
material appears different (Ref.32).

The rate of heat exchanged by the sample including the effect of internal ice
melting may be obtained also from the thermograms and from eq.1 and eq.15 as
shown in the appendix. For a given WSL formed of n_1 and n_w moles of lipid
and water respectively this rate is equal to :

$$\left(\frac{dQ}{dt}\right)_{p_o,n_1,n_w} = \dot{T}_p \left\{ C_{p_o,A,h_w} - 2T \left(\frac{\partial\sigma}{\partial T}\right)_{A,p_o,h_w} \frac{dA}{dT} + \right.$$
$$\left. + AT \left(\frac{\partial\Pi}{\partial T}\right)_{A,p_o,h_w} \frac{dh_w}{dT} + \frac{m_s L}{18\alpha} \left[\frac{\phi(L/1)}{\phi(L/2)} (-\hat{T}_{min})\right]^{1/\alpha} (-\hat{T})^{-\frac{(\alpha+1)}{\alpha}} \right\} = \epsilon \qquad (24)$$

The first term on the r.h.s of (24) is the contribution of the sample heat
capacity outside of the range of phase transition temperatures. This heat
capacity is defined at constant external pressure and constant sample
area A and aqueous spacing h_w. It is known that the contribution of the C_p
term is negligible in the range of phase transition temperatures. Then the
plot of log $(dQ/dt)_{p_o,n_1,n_w}$ vs log $(-\hat{T})$ is linear provided that according to
eq.24 there is no other heat contribution except ice melting i.e. WSL expands
neither laterally (constant A) nor normally (constant h_w). Fully hydrated
lamellar DPPC in the "gel" state (Fig.7) provides such plots. From the best
lines we obtain $2.02 < \alpha < 2.10$ where α is the exponent of the distance power
law for the surface forces (eq.9). The two lines in Fig.7 correspond to two
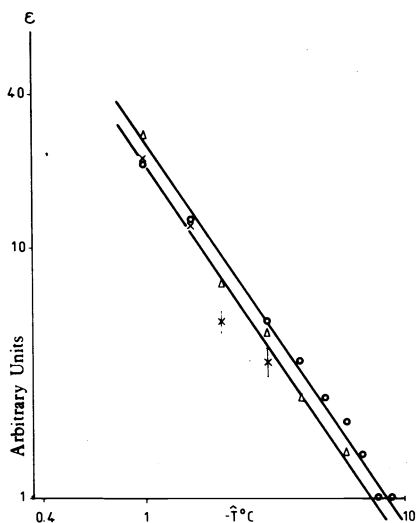scanning rates $\dot{T}_p$ as predicted by eq.24.

Fig.7. Log-log plot of thermo-
grams according to eq.15.
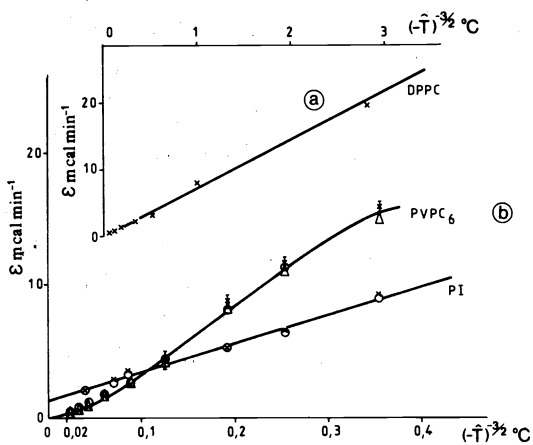DPPC fully hydrated (50%, w/w).

Fig.8. Plot of thermograms according
to eq.15. ε : differential power
input ; - T : ice fusion temperature
depression.
a) Fully hydrated DPPC (50%, w/w).
b) Polysoap PVPC6 + H_2O (60% water
w/w) and fully hydrated PI + H_2O (60%
water w/w).

WSL in the fluid state above the gel-liquid crystal transition temperature
does not provide linear log (dQ/dt) vs log ($\hat{T}$) plots. Assuming the same
mechanism of internal ice melting and the same surface force for fluid and
for "gel" type WSL, we let α = 2 in eq.24 and plot (dQ/dt) vs $(-\hat{T})^{-3/2}$ for PI.
Examples of such plots of thermograms obtained below 0°C are shown in Fig.8
for the rigid bilayers DPPC, for the fluid PI above its transition tempera-
ture ($\sim$ -22.5°C ± 1.5) and for PVPC6 which does not form a multilamellar
phase. Examples of such plots for thermograms obtained below 0°C with the
rigid bilayers of DPPC, with the fluid bilayers of PI and with PVPC6 are
shown in Fig.8. For the rigid DPPC bilayers the contributions of WSL heat of
expansion (second and third term on r.h.s. of 24) seem indeed negligible. For
the fluid bilayers of PI, the plateaus on the thermograms in Fig.9 and the
ordinate at the origin of the line for PI in Fig.8 indicate that an addi-
tional constant rate of heat absorption by the WSL takes place in the range
of internal ice melting temperature. We assume that this rate of heat absorb-
tion parallel to internal ice melting may correspond to WSL expansion : i.e.
dA > 0, (dσ/dt) < 0 and eventually dh_w > 0 in eq.24. At present no results
for ($\partial\Pi/\partial t$) are available.

On the thermograms shown in Fig.9 the peaks for PI gel-liquid crystal and
ice water transitions are distinct. They are separated by plateaus corres-
ponding to the constant rate of heat absorption possibly due to WSL thermal
expansion. At the lowest hydration level (15% H_2O, w/w) the ice melting peak
has vanished, but the constant rate of heat absorption persists. Increasing
the amount of water in the mixture, increases this effect which may become
parallel to internal ice melting (40% H_2O and 60% H_2O w/w in Fig.9). The
fluid bilayers of EL behave in the same way as the fluid PI (see Fig.6). The
EL thermograms provide good plots (not shown) according to eq.24. The
plateaus of the thermograms for PI in Fig.6b become the ordinates at the
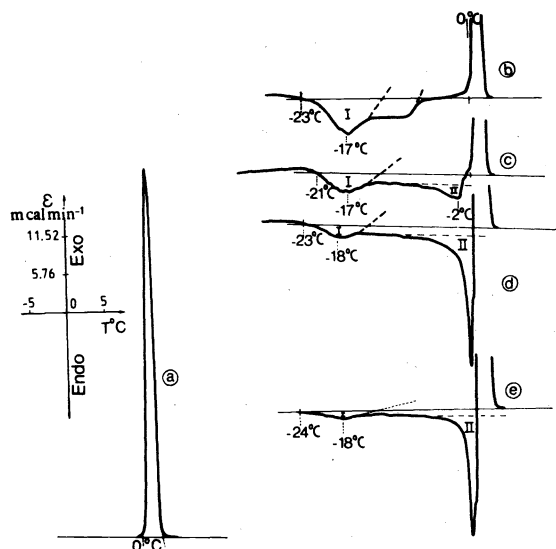origin of the plots ε vs $(-T)^{-3/2}$. An example is shown in Fig.8b.

Fig.9. Thermograms for PI.
Heating rate : $2°$ min^{-1}.
a) Ice melting in reference
cup ; 0.44 mg water ; sample
cup empty.
b) Water 15% (w/w) in sample
cup ; reference cup as in (a)
(2.5 mg PI + 0.44 mg H_2O).
c) Water 20% (w/w) in sample
cup (1.94 mg PI + 0.480 mg H_2O)
Reference cup 0.5 mg H_2O.
d) Water 40% (w/w) in sample
cup (1.52 mg PI + 1.020 mg
H_2O); reference cup 1.02 mg
H_2O.
e) Water 60% (w/w) in sample
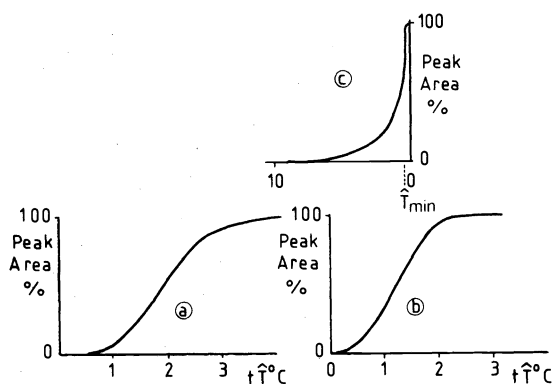cup (1.18 mg PI + 1.89 mg H_2O);
1.9 mg H_2O in reference cup.

Fig.10. Test of cooperativity of
various transitions. Percentage of
peak area vs temperature.
a) Pure ice fusion.
b) DPPC "chain melting" transition.
c) Endothermic peak for "ice" fusion
inside a multilamellar phase of
fully hydrated (50% w/w) DPPC.

The cumulated peak areas corresponding to the heat Q absorbed up to a given
temperature T during a phase transition are shown in Fig.10 for ice melting
in the reference cup R, in the sample S and for the gel-liquid crystal tran-
sition of DPPC bilayers.

TABLE 2. Enthalpies of lipid phase transition and expansion. Internal
water and "non-freezing" water.

System	H_2O%	x_{lip}	ΔH_{lip}	$\Delta H''_{lip}$	H_2O/molecule (mol/mol)		H_2O/molecule (Ref.3 & 4)
			Cal/mol		internal	non-freez	
DPPC	50	1	8.60		21	13	$\sim$ 19
DPPC + PVPC6	50	0.5	0.65		29	16	
DPPC + Ch	50	0.5			20	14	$\sim$ 23
DPPC + VLB	50	0.5	8.0		38	14	
PI	40	1.0	10.5	6.5	22	15	
PI	60	1.0	10.5	6.7	40	32	
PI + PVPC6	40	0.5	0.2		21	2	
EL	50	1.0			39	22	33
EL + Ch	50	0.5			26	16.4	22
PVPC6	50	0.0			16	7	
Ch	50	0.0	0.9(37°C)		9	5.0	

x_{lip} = mol fraction of lipid in the dry mixture ; ΔH_{lip} = molar enthalpy of "gel"-liquid crystal transition ; $\Delta H''_{lip}$ = enthalpy of bilayer expansion (per mol of lipid). (H_2O/molecule)internal : water molecules in the aqueous space per bilayer molecule ; non-freez(ing) water molecules per bilayer molecule defined according to Ref.6. Water molecules per bilayer molecule from X-Ray measurement of the aqueous space width. Temperature cholesterol transition (37°C) at the peak maximum.

In Table 2 we reproduce the molar enthalpy (per lipid molecule) of the low temperature transition of the bilayers ΔH_{lip}. This quantity includes the eventual heat of area A and spacing h_W expansion defined by eq.24. The bilayers are formed either by pure lipids or by lipids + contaminants. Only the results for the composition (1/1), (lipid/contaminant) are shown.

$\hat{T}_f$, $\hat{T}_{min}$, $\hat{T}_{max}$, depressions. Apparent enthalpy of internal ice melting. The depression $\hat{T}_f$ of the nucleation of internal "ice" between bilayers is equal to -21.5°C ± 1.5. For the mixed (1/1)(DPPC/VLB) bilayers $\hat{T}_f$ becomes equal to -22°C ± 1 . This variation is not significant. From the data in Ref.32 for the molar enthalpy of bulk ice melting L = 1150 Cal and for the ice water interfacial tension $\sigma_{iw} \simeq 37$ mNm^{-1} we obtain R = 3.4 nm. This result is of correct order of magnitude. It is strongly dependent on the value used for σ_{iw}. The exothermic peak corresponding to freezing of water and the endothermic peak obtained on ice melting are practically equal (Fig.4, Fig.6) in size although their shapes are very different. The value of (l_0/L),the minimum relative "thickness" of non-freezable water,is obtained from (13c) with α = 2 and $\phi(L/2)$ = 2. The aqueous spacing width h_W = L is proportional to the mass m_S of the aqueous spacing on the number of internal water molecules per bilayer molecule,reported in Table 2. The value of l_0 expressed in the same units is shown in Table 3.

TABLE 3. Non-freezing water molecules and enthalpy of internal ice melting.

System	$-\hat{T}_{min}$ °C	$-\hat{T}_{max}$ °C	m_S mg	Q mcal	non-freez l_0 mol/mol	L cal/mol
DPPC	0.5-0.75	10-12	0.35	12	1.7	743
DPPC/PVPC6 (1/1)	0.5-1	6	0.31	4.2	3.4	324
DPPC/Ch (1/1)	0.5	12.5	0.34	8.4	1.4	517
PI	1	10	1.2	20.5	4.4	394
PI + PVPC6 (1/1)	1.5	16.5	0.82	51	2.0	1430
EL	0.25	16.5	0.45	13.5	1.7	587
EL + Ch (1/1)	0.5	11	0.41	9.4	2.0	486

DPPC and EL containing system have 50% (w/w) water. Those containing PI have 60% (w/w) water for pure PI and 40% water for PI + PVPC6. $\hat{T}_{min}$, $\hat{T}_{max}$ (see eq.13a and 13b). m_S, Q obtained from $\Sigma_{H_2O}^{ref}$ and $\Sigma_{H_2O}^{S}$ as explained in the text. Non-freez l_0 : number of non-freezing water molecules/molecule of bilayer. L = molar enthalpy of water freezing or ice melting inside the aqueous separation.

From the values of l_0 and eq.16 we deduce L the molar enthalpy of "ice" melting inside the aqueous spacing between bilayers. The values of L for various systems are reported in Table 3. Note that $\hat{T}_{min}$, $\hat{T}_{max}$, Q and m_S are measured independently using the peaks S and R respectively of a heating thermogram below and at 0°C (Fig.4, Fig.5, Fig.6 & Fig.9).

DISCUSSION OF THE RESULTS

The osmotic pressure "of a solution" at a given T and the depression of the pure solvent solid-liquid transition temperature at a given p_0 are shifts of intensive parameters, respectively $\delta p = \hat{p}$ and $\delta T = \hat{T}$. These shifts do not affect the thermodynamic properties of the system. They are determined by the additional pressure to be applied on/and by the final temperature of/the

system which allow it (the system) to be in equilibrium with a separated phase of pure solvent (Ref.34). *The shifts $\hat{p}$ and $\hat{T}$ are the result of the lowering of solvent free energy by the solute.* Surface forces affect the free energy and the thermal behaviour (Ref.27, 36 & 37) of "vicinal" water (Ref.38) near surfaces and inside "porous" systems (Ref.21, 32, 35, 36 & 37).

$\hat{p}$ experiments.

In Fig.1 and in eq.1 to eq.8 we undertake a discussion of the ultrafiltration dehydration, or squeezing out of water from the phospholipid "onions" formed by WSL above the gel-liquid crystal transition temperature of the lipid. The measurements (Ref.1-4) provide the value of the flow work for dehydration (eq.8) which has two contributions related to the two origins of the squeezed out δn_W molecules. These origins are the adsorbed n_W^σ and the gap water, inside $h_W = L$ in Fig.1b. Therefore the flow work $v\delta p$ has an interfacial or lateral component significant when the bilayers adsorb water $n_W^\sigma \neq 0$ and when the interfacial tension varies $\delta\sigma \neq 0$. The normal component is significant when $(\partial\Pi/\partial n_W) \neq 0$ and $\delta h_W \neq 0$. These two components have been measured and reported in Ref.3 & 4. The lateral "pressure" defined in Ref.29 becomes here the change $\delta\sigma$ associated with both water adsorption and change in bilayer area A because water molecules act here as spacers (Ref.13, 16 & 17) of lipid molecules. At constant n_l the molecular lipid area (eq.A7) ω_l' and the lipid chemical potential μ_l are modified by water desorption (eq.16) as follows :

$$\delta\mu_{l_{T,p,n_l,\mu_W}} = -\Pi\delta h_W - 2\,\omega_l'\delta\sigma \tag{25}$$

in which the interfacial tension determines the lateral flow work contribution.

A two-dimensional ultrafiltration experiment and the monolayer model of interfaces demonstrate eq.17, eq.18 that surface pressure is different conceptually from the lateral pressure [(eq.8) and (eq.25)]. They have in common the "spacing" parameter for one water molecule (eq.A6) and (eq.20), ω_W, which is the water partial molecular area or water contribution to the monolayer and to the bilayer area A (Ref.39). Values reported for ω_W in the monolayer model are in the range 0.06 sq nm - 0.07 sq nm (Ref.20 & 40).

$\hat{T}$ experiments.

The broad, non-cooperative peaks obtained for water melting inside WSL in contrast to the sharp, cooperative melting peaks of reference water reveal the effect of bilayer surface forces on the free energy of internal water (Figs.4, 5, 6, 9 & 10). Such free energy changes may also be involved by water soluble contaminants or when the "pore" size is not uniform (Ref.31, 32 & 41).

Soluble contaminants and a distribution of "pore" size would produce broad peaks for both ice melting and water freezing in WSL. In contrast, we find *broad* melting peaks associated to *sharp* freezing peaks (Fig.4) in WSL. Located at very different temperatures and different in shape, the melting and the freezing peaks provide the same areas (heats) implying that the same amount of water is involved in both processes. These are shown in Fig.3. Freezing corresponds to ice nucleation inside the aqueous gap. The evaluation of nucleus radius $R < L/2$ using eq.21 and the values for bulk ice water molar enthalpy of transition L and interfacial tension σ_{iw} leads only to a correct order of magnitude for R. However both L and σ_{iw} values might be different for gap and for bulk water. Finally X-Ray experiments have shown that the aqueous gap width is very uniform in multilamellar WSL (Ref.1-4, 22 & 23). The few X-Ray experiments carried out at low temperatures have shown that in the gel state the distance parameters are not affected by the temperature (Ref.23). Therefore neither contaminants nor "pore" size heterogeneity can explain the DSC melting and freezing thermograms of WSL. Surface forces are more successful (Ref.21 and eq.9, eq.13, eq.15, eq.16 & eq.24).

An ice melting peak inside WSL is limited by a low temperature shift $\hat{T}_{max}$ and a high temperature shift $\hat{T}_{min}$ (Fig.4). They are both dependent on the bilayer surface forces (eq.13a and eq.13b). Moreover, $\hat{T}_{max}$ depends on the thickness l_o (Ref.21) of the non-freezing water while $\hat{T}_{min}$ depends on the aqueous gap width L (Fig.2). The ratio $(\hat{T}_{max}/\hat{T}_{min})$ also depends on the surface forces (power α) and on the relative value (l_o/L) (eq.13c).

When neither bilayer area A nor aqueous gap width L vary with temperature, the shape of the ice melting peak is given by eq.15. In the limit $(l \rightarrow l_o)$

when $\{\phi(1/L)/\phi(L/2)\} \simeq$ const,a log ε log $(-\hat{T})$ plot of the thermogram pro-
vides the value of α. The rigid DPPC bilayers verify this thermogram (Fig.5
& 7). The value α = 2 thus obtained is the power in the expression of surface
forces (eq.9) and (Ref.21 & 27). Such a log ε log $(-\hat{T})$ plot is not linear
when the WSL expands on heating (eq.24). Using the value α = 2 linear plots
of the power ε vs $(-\hat{T})^{-3/2}$ are obtained which extrapolate to $\varepsilon_0 \neq 0$ when
$\hat{T} \to \hat{T}_{max}$. The value of ε_0 is the power absorbed by the WSL to modify its
bilayer area A and aqueous gap h_w when heated. Such effects correspond to the
"plateaus" on the thermograms and are obtained only with "fluid" bilayers of
WSL such as PI, EL (see Fig.6, 8 & 9) and DPPC/Ch (1/1) (not shown). For PI
the heat of expansion $\Delta H''_{lip}$ (Table 1) is about 60% of the heat of gel-liquid
crystal transition. It is important to note that this expansion is parallel
to ice "melting" i.e. to water becoming available inside the aqueous gap.

The mass of internal water inside the aqueous gap of various lamellar systems
is obtained from the area of the ice melting peak in the reference R (Table 2)
and Table 3). Our results (Table 2) are close to those obtained by X-Ray
studies (last column). We note that the positively charged polysoap (PVPC6)
and drug (VLB) which fluidify the rigid DPPC bilayers (Ref.21 & 33), increase
considerably the hydration of the WSL i.e. the amount of internal water.
Cholesterol does not seem to have such an effect on DPPC (preliminary
results). In contrast, it apparently dehydrates the fluid EL.

It is interesting to compare these results with the hydration of the pure
constituents of mixed bilayers. PVPC6 and Ch are poorly hydrated. Careful
analysis of results recquires the ideal (mean) molecular hydration number for
a mixed bilayer to be compared to the experimental results. From column 5 of
Table 2 we obtain for the ideal (DPPC + Ch) (1/1) and (EL + Ch) (1/1) the
values 14.5 and 24 (water molecules)/(molecule of bilayer). The well known
fluidifying effect of cholesterol is accompanied by a 30% increase in
hydration of DPPC bilayers. It is evident from Table 2, that hydration of
WSL fluid bilayers is always superior to that of rigid ones (compare DPPC
with EL and PI).

The heat of ice melting of the internal water Q (in Table 3) is obtained
independently of the value of its mass m_s. It corresponds to the melting of
a mass of water smaller than m_s (eq.16) by a percentage given by $(2l_0/L)$.
This percentage is obtained independently from the limits $\hat{T}_{min}$ and $\hat{T}_{max}$ of
the internal ice melting peaks (eq.13c). Using the values of L given in
column 5 of Table 2, the number of non-freezing molecules equivalent to l_0
is deduced and reported in Table 3, column 6. From m_s, Q, (l_0/L) and eq.16
we obtain L, the heat of melting. These values are independent of any
assumption on the state of water molecules inside the aqueous gap separating
the bilayers of Fig.1. Our present method for finding out the non-freezing
number of water molecules l_0 is original and different from that in Ref.6 &
21. In addition we provide the value of the molar enthalpy of "melting" L of
internal ice, which has been assumed equal to that of bulk ice in Ref.6. The
results obtained using this last assumption are shown in Table 2, column 6.
They are much higher than those obtained by the present approach (l_0) in
Table 3. The last results show also that the uncharged cholesterol does not
modify significantly the number of strongly perturbed or non-freezing water
molecules in contrast to the effect of the charged PVPC6 which "hydrates" the
amphoteric DPPC and dehydrates the charged acidic PI (Table 3). These results
qualitatively agree with those obtained previously. However, in addition, we
show (Table 3, last column) that the heat of the non-cooperative ice melting
(Fig.10) decreases in an extent which increases with the charge of the
bilayer and, presumably, with the strength of the surface forces field. Thus
when surfaces are charged (PI and DPPC + PVPC6) the molar enthalpy L is
smallest : about 25% of the bulk value of L. When the charges are neutralized
it increases to the bulk value (see PI + PVPC6 result, Table 3).

The values of L we obtain are average values over the gap L. Our method does
not allow the resolve the variation of L with distance y from the water
bilayer interface inside the aqueous gap. It shows though that surface fields
may perturb them strongly. The values for the number of non-freezing water
molecules are smaller than the ones reported in Ref.6 & 21. They are closer
to the number of water molecules acting as spacers of lipid molecules in
bilayers (Ref.16) and probably located between their polar heads. The
parallel effects of electrostatic interaction on hydration of mixed bilayers
and condensation in mixed films have been shown in Ref.21 for the first
time.

CONCLUSION

To understand the process of ice melting inside the aqueous gaps between lipid bilayers the mass of ice and its molar enthalpy of melting have to be determined independently. This is possible using the present interpretation of the melting thermograms. The value of L and the cooperativity are controlled by the fluidity and the charge of the bilayers by means of their field of surface forces. Cooperativity of ice melting process is abolished, because it has to start at the bilayer ice interface. In contrast, nucleation of ice is still cooperative, but the molar enthalpies of this process and of melting are equal indicating that the surface forces bring the molar entropies of internal ice and water closer. While the bilayers control the ice melting process, ice nucleation has preserved its autonomy.

ANNEX

In general, for the parameters appearing in eq.1 and characterizing the WSL, given n_1, n_w, the heat exchanged is equal to :

$$(TdS)_{n_1,n_w} = T(\frac{\partial S}{\partial T})_{p,A,h_w} \, dT + T(\frac{\partial S}{\partial p})_{T,A,h_w} \, dp + T(\frac{\partial S}{\partial A})_{T,p,h_w} \, dA +$$
$$+ T(\frac{\partial S}{\partial h_w})_{T,p,A} \, dh_w \tag{A1}$$

When the function $\tilde{G} = U + pV - TS$ appearing in (2) is used to eliminate dU of eq.1, it is obtained :

$$d\tilde{G} = - SdT + Vdp + 2\sigma dA - A\Pi dh_w + \mu_1 dn_1 + \mu_w dn_w \tag{A2}$$

Maxwell cross differentiation of the coefficients in A2 provides the partial derivatives appearing in (24) :

$$(TdS)_{n_1,n_w} = C_{A,h_w,p} \, dT - T(\frac{\partial V}{\partial T})_{p,A,h_w} \, dp - 2T(\frac{\partial \sigma}{\partial T})_{A,p,h_w} \, dA +$$
$$+ AT(\frac{\partial \Pi}{\partial T})_{p,A,h_w} \, dh_w \tag{A3}$$

The heat capacity is defined at a given pressure p_0, internal area A and aqueous spacing. In the range of temperature where the ice water phase transition occurs, the total heat exchanged by the sample is obtained by adding to (A3) the contribution predicted by eq.15. Then we get at constant pressure the following predicted rate of heat exchanged by the sample :

$$(\frac{dQ}{dt})_{p_0,n_1,n_w} = \dot{T}_p \{C_{p_0,A,h_w} - 2T(\frac{\partial \sigma}{\partial T})_{A,p_0,h_w} \frac{dA}{dT} + AT(\frac{\partial \Pi}{\partial T})_{A,p_0,h_w} \frac{dh_w}{dT} +$$
$$+ \frac{m_s L}{18\alpha} \{\frac{\phi(1/L)}{\phi(L/2)} \, (-\hat{T}_{min})^{1/\alpha}\}(-\hat{T})^{-(\alpha+1)/\alpha}\} \tag{A4}$$

From (2) and (A2) the following Gibbs-Duhem equation is deduced :

$$SdT - Vdp + A\Pi dh_w + n_w \, d\mu_w + n_1 \, d\mu_1 + 2Ad\sigma = 0 \tag{A5}$$

For the ultra filtration at constant T, μ_w, n_1, n_w, p_0 and $p_0 + \delta p$ (A5) becomes :

$$\Pi dh_w + 2 \, \omega_1' \, d\sigma + d_{T,p} \, \mu_1 = 0 \tag{A6}$$

where ω_1' defined as follows :

$$\omega_1' = (A/n_1)_{T,p,\sigma} \tag{A7}$$

is the area per molecule of bilayer.

REFERENCES

1. D. Le Neveu, R.P. Rand and A.V. Parsegian, Nature, 259, 601-603 (1976).
2. D. Le Neveu, R.P. Rand, A.V. Parsegian and D. Gingell, Biophys. J., 18, 203-209 (1977).
3. A.V. Parsegian, N. Fuller and R.P. Rand, Biochemistry, 76, 2750-2754 (1979).
4. R.P. Rand, Ann. Rev. Biophys. Bioeng., 10, 277-314 (1981).
5. D. Chapman, R.M. Williams and B.D. Ladbrooke, Chem. Phys. Lipids, 1, 445-475 (1967).
6. B.D. Ladbrooke, R.M. Williams and D. Chapman, Biochim. Biophys. Acta, 150, 333-340 (1968).
7. D. Chapman, Form and Function of Phospholipids, Eds. G.B. Ansell, J.N. Hawthorne, R.M.C. Dawson, Elsevier, Amsterdam (1973); Q. Rev. Biophys., 8, 185-235 (1975).
8. J. Seelig and A. Seelig, Q. Rev. Biophys., 13, 19-61 (1980).
9. A.G. Lee, Biochim. Biophys. Acta, 472, 285-344 (1977).
10. H.V. Gally, A. Seelig and J. Seelig, Hoppe Seyler's Z. Physiol. Chem., 357, 1447-1450 (1976).
11. B.A. Cornell, M. Keniry, R.G. Hiller and R. Smith, FEBS Letts., 115, 134-138, 1980.
12. E. Bricknell-Brown and K.G. Brown, Biochem. Biophys. Res. Commun., 94, 638-645 (1980).
13. S. Fowler Bush, H. Levin and I.W. Levin, Chem. Phys. Lipids, 27, 101-111 (1980)
14. H. Brockerhoff, Bioorganic Chemistry, III, Macro and Multimolecular Systems, Acad. Press, N-Y., 1-20 (1977).
15. N.K. Ayengar, L.C. Lipton and H. Brockerhoff, Chem. Phys. Lipids, 25, 203-208 (1979).
16. G. Büldt, H.V. Gally, A. Seelig, J. Seelig and G. Zaccai, Nature, 271, 182-184 (1978).
17. J.C.W. Shepherd and G. Büldt, Biochim. Biophys. Acta, 558, 41-47 (1979).
18. F. Müller-Landau and D.A. Cadenhead, Chem. Phys. Lipids, 25, 299-314, 315-328, 329-343 (1979).
19. R.A. Demel and B. Kruyff, Biochim. Biophys. Acta, 457, 109-132 (1976).
20. H. Steinbach and Ch. Sucker, Colloid & Polymer Sci., 257, 192-200 (1975).
21. L. Ter-Minassian-Saraga and G. Madelmont, J. Colloid & Interf. Sci., in press.
22. V. Luzzati, Biological Membranes, Ed. D. Chapman, 1, 71-123, Acad. Press, London (1968).
23. J.L. Ranck, R. Keira and V. Luzzati, Biochim. Biophys. Acta, 488, 432-441 (1977).
24. G. Zaccai and D.J. Gilmore, J. Mol. Biol., 132, 181-191 (1979).
25. P.K. Rogan and G. Zaccai, J. Mol. Biol., 145, 281-283 (1981).
26. R. Defay, I. Prigogine, A. Bellemans and E.H. Everett, Surface Tension and Adsorption, Longmans, London (1966).
27. R.P. Gilpin, J. Colloid & Interf. Sci., 68, 235-251 (1979).
28. Handbook of Chemistry and Physics, 59th Ed., CRC Press, USA, B272 (1978-1979).
29. S. Marcelja, Biochim. Biophys. Acta, 367, 165-176 (1974).
30. A. Scheludko, Colloid Chemistry, Elsevier, Amsterdam, Ch.IV, 2, p.98 (1966).
31. W. Kuhn, Helv. Chim. Acta, Vol.39, Fasc.4, 128, 1071-1086 (1956).
32. M. Brun, A. Lallemand, G. Lorette, J.F. Quinson, M. Richard, L. Eyraud and C. Eyraud, J. Chim. Phys., 70, 973-978, 979-989, 990-996 (1973); Thermochim. Acta, 21, 59-88 (1977).
33. L. Ter-Minassian-Saraga, G. Madelmont, C. Hort-Legrand and S. Métral, Biochem. Pharm., 30, 411-415 (1980).
34. E.A. Guggenheim, Thermodynamics, North-Holland, Amsterdam, 194 (1949).
35. S.S. Barer, B. Derjaguin, O.A. Kiseleva, V.D. Sobolev and N.V. Churaev, Kolloid Zhurn., 39, 1039 (1977).
36. S.S. Barer, N.V. Churaev, B. Derjaguin, O.A. Kiseleva and V.D. Sobolev, J. Colloid & Interf. Sci., 74, 173-180 (1980).
37. M. Vignes, J. Colloid & Interf. Sci., 60, 162-171 (1977).
38. W. Drost-Hansen, Phys. Chem. Liq., 7, 243-348 (1978).
39. L. Saraga and I. Prigogine, Comptes Rendus de la 2ème Réunion de Chim. Phys., Ed. Soc. Chim. Phys. Paris, 458-462, 2-7 juin (1952).
40. L. Ter-Minassian-Saraga and I. Prigogine, Mém. Serv. Chim. de l'Etat, 38, 2, 109-124 (1953).
41. D.H. Everett, Trans. Farad. Soc., 57, 1541-1551 (1961).